Nanostructures

DOI: 10.1002/anie.201008224

Encapsulation of Nanoparticles in Block Copolymer Micellar Aggregates by Directed Supramolecular Assembly**

*Weikun Li, Shanqin Liu, Renhua Deng, and Jintao Zhu**

Incorporation of inorganic nanoparticles (NPs) into self-assembled block copolymers offers a powerful route for the formation of hybrid materials with desired optical, electronic, and magnetic properties through the choice of NPs and their distribution in polymer assemblies.[1–4] Nanostructured block copolymer domains act as a scaffold that directs not only the position of the NPs but also their orientation.[5–9] NPs/polymer hybrid materials have been prepared in solution by incorporating one or multiple hydrophobic NPs into a hydrophobic core of spherical amphiphilic block copolymer micelles.[10–13] Careful control of micellization conditions will allow other hydrophobic ingredients to co-assemble with the amphiphilic polymers, resulting in micelles that encapsulate therapeutic molecules and NPs for imaging and targeting.[14]

Cylindrical or wormlike micelles show particular interest in drug delivery because of their large core volume (per carrier) and elongated structures, which offer additional opportunities to control biodistribution and release profiles of therapeutic agents.[15] The "precipitation method", which is a practical way to incorporate NPs into micelles,[10–13] does not easily allow the growth of extended wormlike micelles with NPs encapsulated in the core. Several groups have reported the successful incorporation of NPs into hydrophilic portions of wormlike micelles through electrostatic interaction of corona-forming blocks with NPs.[16,17] Recently, we reported the encapsulation of iron oxide NPs within wormlike micelle cores through interfacial instabilities of emulsion droplets containing amphiphilic polymers.[18] However, it is hard to achieve high loading and uniform dispersion of NPs in wormlike micelle cores.[14,18] So far, precise control over NPs position in wormlike micelle cores with homogeneous distribution remains a challenge.

Herein we introduce a simple, yet versatile approach for the encapsulation of NPs within wormlike micelle cores through directed supramolecular assembly. The concept for preparation of the hybrid nano-objects is illustrated in Figure 1 a. Typically, polystyrene–poly(4-vinylpyridine) (PS_{20k}–$P4VP_{17k}$, volume fraction of PS $\phi_{PS} = 56\,\%$) and pentadecylphenol (PDP) were dissolved in chloroform to form PS–P4VP(PDP)$_x$ (x represents the ratio of PDP to 4VP units) comb–coil supramolecules, which can further self-assemble into hierarchical structures.[19] Monodisperse gold NPs [size: (6.5 ± 0.7) nm] were synthesized and functionalized with a thiol-end PS_{2k} (see the Supporting Information for experimental details, as well as Figure S1 and Table S1 in the Supporting Information).[20] Upon addition of PS_{2k}-coated NPs to the supramolecules, hierarchical structures—in which gold NPs were selectively incorporated in cylindrical PS phases within P4VP(PDP)$_{1.0}$ matrices (Figure S2 in the Supporting Information) owing to preferential interaction of the NPs with the PS block and unfavorable interaction of the NPs with the P4VP(PDP) domain—were obtained after slow evaporation of the organic solvent. Isolated wormlike micelles with uniformly dispersed gold NPs along the centerline were obtained by removal of small-molecule PDP (Figure 1 b).[21] The hybrid nano-objects have a core–corona structure with a PS/NPs core and P4VP chains as a corona, thus increasing solubility and providing stability of the nano-

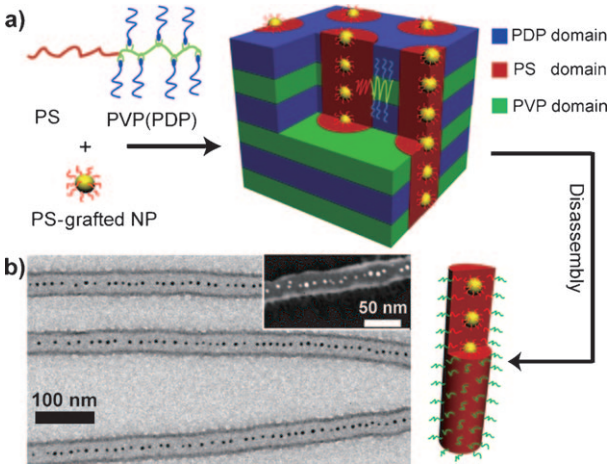

Figure 1. a) Illustration of comb–coil supramolecules based on PS_{20k}–$P4VP_{17k}$ (PDP)$_{1.0}$ ($\phi_{PS} = 23\,\%$), in which PDP hydrogen-bonds to P4VP; the hierarchical structures were formed by assembly of the supramolecules and NPs; isolated hybrid micelles were obtained from disassembly of the supramolecules by dialysis against alcohol to rupture the hydrogen-bonding. b) Bright-field TEM image of isolated PS_{20k}–$P4VP_{17k}$ wormlike micelles encapsulated with 6.5 nm NPs; the inset shows the dark-field TEM image (also see Figure S3 in the Supporting Information).

[*] W. K. Li, S. Q. Liu, R. H. Deng, Prof. J. T. Zhu
Hubei Key Lab of Materials Chemistry & Service Failure
School of Chemistry & Chemical Engineering
Huazhong University of Science and Technology
Wuhan, Hubei, 430074 China
Fax: (+86) 27-875-43632
E-mail: jtzhu@mail.hust.edu.cn

[**] We gratefully acknowledge funding for this work provided by the National Science Foundation of China (21004025) and the Chinese Ministry of Education with the Program of New Century Excellent Talents in University (NCET-10-0398), and initiatory financial support from HUST. We also thank HUST Analytical and Testing Center for allowing us to use its facilities.

Supporting information for this article is available on the WWW under http://dx.doi.org/10.1002/anie.201008224.

objects in alcohol. We demonstrate that interparticle spacing and micellar morphology can be readily tailored by varying the NP or PDP content. The current approach offers a simple route for encapsulation of NPs within the micellar core that may present new opportunities for applications in drug delivery, targeting, and diagnosis.[11,22,23]

The controlled manipulation of interparticle spacing provides new dimensionality to influence the optical and magnetic properties of NPs.[1,24] As shown in the insets of Figure 2, 6.5 nm NPs (in what follows, we refer to PS-coated

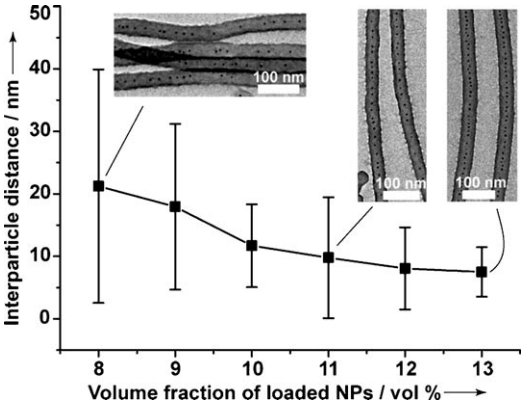

Figure 2. Relationship between interparticle distance and volume fraction (ϕ_{NP}). NP size, interparticle distance, and ϕ_{NP} were obtained based on TEM images and results of thermal gravimetric analysis (see Tables S1 and S2 in the Supporting Information). The inset shows representative TEM images for the hybrid wormlike micelles from PS_{20k}–$P4VP_{17k}$ $(PDP)_{1.0}$ with 6.5 nm NPs. The standard deviation, indicated by error bars, decreased when ϕ_{NP} increased to 13%, indicating relatively uniform dispersion of NPs in micelles.

NPs as NPs for conciseness) were dispersed selectively within the center of wormlike micelle cores in a single line. Moreover, the mean interparticle distance decreased from (21.2 ± 18.6) nm to (7.4 ± 3.9) nm when increasing ϕ_{NP} from 8 to 13%, as confirmed by the increase of the average number of NPs per 100 nm in micelles when increasing ϕ_{NP} (Figure S5 in the Supporting Information). Surface plasmon resonance spectra of the hybrid micelles are red-shifted slightly when interparticle spacing is decreased (Figure S6 in the Supporting Information). In addition, the diameter of the hybrid micelles increases nearly linearly with the increase of ϕ_{NP} (Figure S7 in the Supporting Information). This behavior provides an easy means to control interparticle spacing and could find applications in areas of device fabrication, sensors, and nonlinear optics.[25]

Once ϕ_{NP} increases beyond 13%, the wormlike micelles change to a mixture of wormlike micelles and nanosheets with cylindrical protrusions (Figure 3a, $\phi_{NP} = 15\%$), and then to nanosheets (Figure 3b, $\phi_{NP} = 28\%$). The interparticle distance in the nanosheets was estimated to be 7.0 nm from the area density of NPs in the bilayers, assuming uniform dispersion of NPs. A further increase of ϕ_{NP} to 40% leads to the formation of perforated nanosheets (Figure S9 in the Supporting Information). Selective loading of NPs within PS domains resulted in at least two effects: 1) variation of the

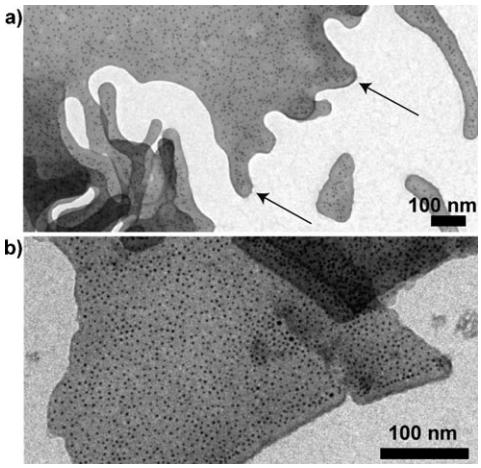

Figure 3. TEM images of a) mixtures of wormlike micelles and nanosheets with cylindrical protrusions (indicated by arrows; also see Figure S8 in the Supporting Information) from PS_{20k}–$P4VP_{17k}$ $(PDP)_{1.0}$ with 6.5 nm NPs ($\phi_{NP} = 15\%$; $\phi_{PS(NP)} = 35\%$); we interpret these structures as a transition of cylinder-to-lamellae. b) Nanosheets from PS_{20k}–$P4VP_{17k}$ $(PDP)_{1.0}$ with 6.5 nm NPs, ($\phi_{NP} = 28\%$; $\phi_{PS(NP)} = 45\%$).

value of ϕ_{PS} similar to incorporated homopolymers; 2) modification of interfacial curvature through variation of chain stretching. All of these effects will drive the supramolecular system to cross the phase boundary to form a new phase with varied morphology and size beyond a critical content.[5,8]

To explore the influence of the NP size on the assembly morphology, we tested several gold NPs with different core sizes [ranging from (1.7 ± 0.8) nm to (18 ± 3.5) nm] at a fixed ϕ_{NP} value of 10%. As shown in Figure 4a, NPs have a homogeneous or broad distribution within wormlike micelle cores when $D/R_0 < 1.0$ (where D is the size of NP core and PS brush, and R_0 is root-mean-square end-to-end distance of PS block[4]; Table S1 in the Supporting Information). However, when the D/R_0 value was varied from 1.11 to 2.12, NPs preferred to locate near the center of PS cylindrical cores (Figure 2 for $D/R_0 = 1.40$ and Figure 4b,c). This trend agrees

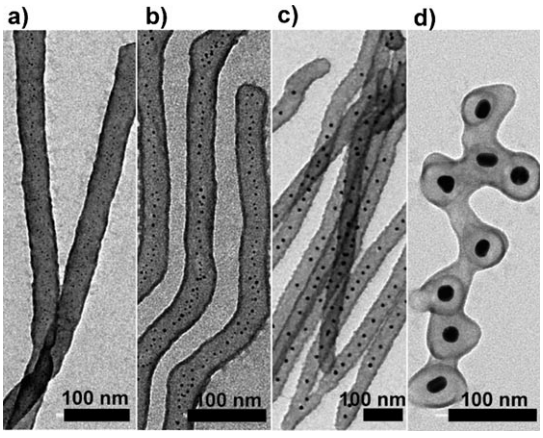

Figure 4. TEM images of wormlike micelles from PS_{20k}–$P4VP_{17k}$ $(PDP)_{1.0}$ with incorporated NPs at a fixed ϕ_{NP} of 10% and NP sizes of: a) 1.7 nm ($D/R_0 = 0.63$); b) 3.5 nm ($D/R_0 = 1.11$); c) 10.5 nm ($D/R_0 = 2.12$); d) 18.0 nm ($D/R_0 = 2.85$).

well with theoretical results, which suggested that large NPs could be found at the center of specific domains whereas small ones have a broader distribution to maximize their entropy because of the greater translational entropy relative to that of large NPs given a fixed value of ϕ_{NP}.[26,27] A further increase of the NP size to 18 nm gives rise to wormlike micelles with undulations in which NPs are located at enlarged points (Figure 4d).

A key advantage of the use of supramolecular assemblies for preparing hybrid micelles is that the composition of the blocks can be easily adjusted by changing the number of side chains while using the same copolymer, thus allowing reversible changes in morphology and its characteristic size. As the PDP/P4VP ratio was increased to 2.0, free PDP could be intercalated between hydrogen-bonded PDP, giving $\phi_{P4VP(PDP)} = 85\%$, and a PS spherical domain embedded in $P4VP(PDP)_{2.0}$ matrix was formed. Figure 5a shows TEM images in which one or more 3.5 nm NPs are encapsulated into a single spherical micelle. The inset shows the distribution of NPs in spherical micelles, showing that most of the micelles incorporated two NPs. However, as the NP size was increased to 10.5 nm, most of the spherical micelles incorporated only one NP along with some empty micelles (Figure 5b, indicated by arrows). The overall dimension of the spherical micelles increased from (31 ± 2.7) to (46 ± 2.6) nm when increasing the NP size (Figure S10 in the Supporting Information).

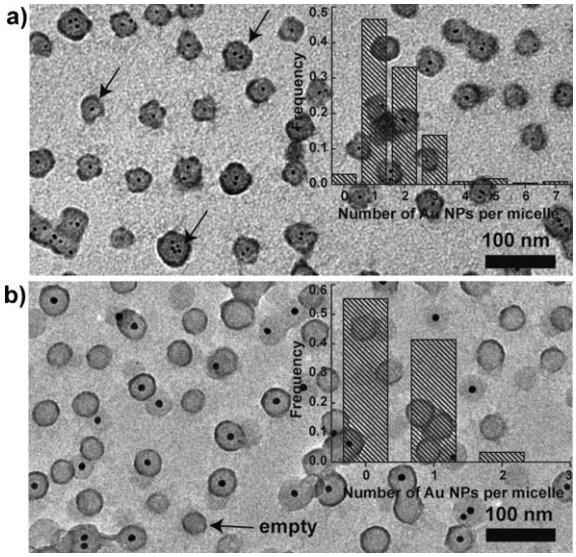

Figure 5. TEM images of spherical micelles from PS_{20k}–$P4VP_{17k}(PDP)_{2.0}$ containing NPs ($\phi_{NP} = 8\%$) with sizes of a) 3.5 nm; b) 10.5 nm.

To test the generality of this approach, we investigated another copolymer, PS_{51k}–$P4VP_{18k}$. Owing to the higher PS content of PS_{51k}–$P4VP_{18k}$ ($\phi_{PS} = 74\%$), the windows in which to tune hybrid micellar morphologies through supramolecular assemblies are broad, covering nanosheets, cylinders, and spheres when varying the PDP content (Figures S11 and S12 in the Supporting Information). Moreover, we tested another supramolecular pair, PS–poly(ethylene oxide) (PS_{38k}–PEO_{11k}, $\phi_{PS} = 80\%$) with dodecylbenzenesulfonic acid, which would hydrogen-bond with the PEO block. Similarly, wormlike micelles with incorporated NPs were obtained when the ϕ_{PS} value was 29% in the supramolecule (Figure S13 in the Supporting Information).

In summary, we have demonstrated the successful encapsulation of NPs in micelle cores through directed supramolecular assembly. Micellar morphologies and interparticle spacing can be readily tailored by varying the PDP and NP content. Our experimental technique can be extended to other supramolecular pairs and NPs of different types (Figure S14 in the Supporting Information). This new approach also provides a platform to fabricate multifunctional micelles by introducing functional NPs with desirable optical, electronic, and magnetic properties into such micelles for diagnostic imaging, drug delivery, sensors, and device fabrication. Further work is required to fully understand the mechanism driving NPs to micelle cores or to broad distribution, and to fully define the roles of graft density, ligands, and NP shape on the encapsulation.

Received: December 28, 2010
Revised: March 31, 2011
Published online: May 10, 2011

Keywords: block copolymers · micelles · nanoparticles · self-assembly · supramolecular chemistry

[1] Z. H. Nie, A. Petukhova, E. Kumacheva, *Nat. Nanotechnol.* **2010**, *5*, 15.
[2] A. C. Balazs, T. Emrick, T. P. Russell, *Science* **2006**, *314*, 1107.
[3] Y. Zhao, K. Thorkelsson, A. J. Mastroianni, T. Schilling, J. M. Luther, B. J. Rancatore, K. Matsunaga, H. Jinnai, Y. Wu, D. Poulsen, J. M. J. Frechet, A. P. Alivisatos, T. Xu, *Nat. Mater.* **2009**, *8*, 979.
[4] S. C. Warren, F. J. Disalvo, U. Wiesner, *Nat. Mater.* **2007**, *6*, 156.
[5] B. J. Kim, J. J. Chiu, G. R. Yi, D. J. Pine, E. J. Kramer, *Adv. Mater.* **2005**, *17*, 2618.
[6] J. J. Chiu, B. J. Kim, E. J. Kramer, D. J. Pine, *J. Am. Chem. Soc.* **2005**, *127*, 5036.
[7] Q. F. Li, J. B. He, E. Glogowski, X. F. Li, J. Wang, T. Emrick, T. P. Russell, *Adv. Mater.* **2008**, *20*, 1462.
[8] S. W. Yeh, K. H. Wei, Y. S. Sun, U. S. Jeng, K. S. Liang, *Macromolecules* **2005**, *38*, 6559.
[9] J. J. Chiu, B. J. Kim, G. R. Yi, J. Bang, E. J. Kramer, D. J. Pine, *Macromolecules* **2007**, *40*, 3361.
[10] Y. J. Kang, T. A. Taton, *Angew. Chem.* **2005**, *117*, 413; *Angew. Chem. Int. Ed.* **2005**, *44*, 409.
[11] H. Ai, C. Flask, B. Weinberg, X. Shuai, M. D. Pagel, D. Farrell, J. Duerk, J. M. Gao, *Adv. Mater.* **2005**, *17*, 1949.
[12] L. E. Euliss, S. G. Grancharov, S. O'Brien, T. J. Deming, G. D. Stucky, C. B. Murray, G. A. Held, *Nano Lett.* **2003**, *3*, 1489.
[13] B. L. Sanchez-Gaytan, W. H. Cui, Y. J. Kim, M. A. Mendez-Polanco, T. V. Duncan, M. Fryd, B. B. Wayland, S. J. Park, *Angew. Chem.* **2007**, *119*, 9395; *Angew. Chem. Int. Ed.* **2007**, *46*, 9235.
[14] R. C. Hayward, D. J. Pochan, *Macromolecules* **2010**, *43*, 3577.
[15] Y. Geng, P. Dalhaimer, S. S. Cai, R. Tsai, M. Tewari, T. Minko, D. E. Discher, *Nat. Nanotechnol.* **2007**, *2*, 249.
[16] H. G. Cui, Z. Y. Chen, S. Zhong, K. L. Wooley, D. J. Pochan, *Science* **2007**, *317*, 647.

[17] H. Wang, W. J. Lin, K. P. Fritz, G. D. Scholes, M. A. Winnik, I. Manners, *J. Am. Chem. Soc.* **2007**, *129*, 12924.
[18] J. T. Zhu, R. C. Hayward, *J. Am. Chem. Soc.* **2008**, *130*, 7496.
[19] O. Ikkala, G. ten Brinke, *Science* **2002**, *295*, 2407.
[20] S. Rucareanu, M. Maccarini, J. L. Shepherd, R. B. Lennox, *J. Mater. Chem.* **2008**, *18*, 5830.
[21] A. W. Fahmi, H. G. Braun, M. Stamm, *Adv. Mater.* **2003**, *15*, 1201.
[22] J. H. Park, G. von Maltzahn, E. Ruoslahti, S. N. Bhatia, M. J. Sailor, *Angew. Chem.* **2008**, *120*, 7394; *Angew. Chem. Int. Ed.* **2008**, *47*, 7284.
[23] H. Wang, J. Xu, J. H. Wang, T. Chen, Y. Wang, Y. W. Tan, H. B. Su, K. L. Chan, H. Y. Chen, *Angew. Chem.* **2010**, *122*, 8604; *Angew. Chem. Int. Ed.* **2010**, *49*, 8426.
[24] R. Shenhar, T. B. Norsten, V. M. Rotello, *Adv. Mater.* **2005**, *17*, 657.
[25] S. K. Ghosh, T. Pal, *Chem. Rev.* **2007**, *107*, 4797.
[26] M. W. Matsen, R. B. Thompson, *Macromolecules* **2008**, *41*, 1853.
[27] M. K. Gaines, S. D. Smith, J. Samseth, M. R. Bockstaller, R. B. Thompson, K. O. Rasmussen, R. J. Spontak, *Soft Matter* **2008**, *4*, 1609.

